Reduction Rate of Iron Oxide Pellets with Hydrogen

Reduction Rate of Iron Oxide Pellets with Hydrogen*

Reijiro TAKAHASHI, Jun-ichiro YAGI and Yasuo OMORI

The Research Institute of Mineral Dressing and Metallurgy

(Received July 7, 1971)

Synopsis

For analyzing the reduction process in the metallurgical reactor, especially in blast furnace, the reduction rates of hematite pellet and iron oxide pellet pre-reduced to wustite, "wustite pellet", were expressed by a mathematical model and the rate parameters thereof were determined.

An unreacted core model was applied to simulate the hydrogen reduction of iron oxide pellets within the temperature range from 850 to 1,150°C. Comparison of the rate constant of chemical reaction and its activation energy of hematite pellet with those of wustite pellet did not show significant difference. The pellets used had an activation energy of about 21 to 26 kcal/mol.

In the macro- and microscopic observation of iron oxide pellets during the reduction, the reaction proceeded topochemically. A sharp interface was found between wustite and iron phase in the case of hematite pellet, whereas reaction zone of about 300 μ was found in the case of wustite pellet.

The calculated reduction curves almost agreed with the observed values with the changes of temperatures, diameters of the pellet and concentrations of reducing gas. These calculated curves further agreed with the values observed by altering one of the experimental conditions during reduction.

I. Introduction

Theories of rate control for the gaseous reduction of iron oxides include the analysis based on an assumption of a single rate controlling step such as the chemical reaction control proposed by McKewan[1] or the intraparticle diffusion control proposed by von Bogdandy and Janke.[2] In recent years, however, analysis based on the mixed control was proposed, in which diffusion through gaseous film, intraparticle diffusion and chemical reaction processes are taken into account.[3]~[9]

* The **196th** report of the Research Institute of Mineral Dressing and Metallurgy. Originally published in Japanese in Bulletin of the Research Institute of Mineral Dressing and Metallurgy, Tohoku University, **26** (1970), 83 and in Tetsu-to-Hagané, **57** (1971), 1597.

(1) W.M. McKewan: Trans. Met. Soc. AIME, **218** (1960), 2.
(2) L. von Bogdandy and W. Janke: Z. Electrochem., **61** (1957), 1146.
(3) Y. Hara, M. Tsuchiya and S. Kondo: Tetsu-to-Hagané, **55** (1969), 1297.
(4) A. Moriyama, J. Yagi and I. Muchi: Trans. Iron and Steel Inst. Japan, **7** (1967), 271.
(5) T. Yagi and Y. Ono: Trans. Iron and Steel Inst. Japan, **8** (1968), 377.
(6) R.H. Spitzer, F.S. Manning and W.O. Philbrook: Trans. Met. Soc. AIME, **236** (1966), 726.
(7) B. Seth and H.U. Ross: Trans. Met. Soc. AIME, **233** (1965), 180.
(8) J. Feinman, N.D. Smith and D.A. Muskat: Indust. Eng. Chem. Process Design and Development, **4** (1965), 270.
(9) H.W. St. Clair: Trans. Met. Soc. AIME, **233** (1965), 1145.

Rate parameters included in the equation of reduction rate have been decided by using the data of such reactors as fixed and moving beds,[10],[11] or the data of the direct measurement in the blast furnace[12]. In analyzing the reduction process of an iron oxide pellet in a reactor, however, the reduction rate should be expressed in an accurate and relatively simple form and the rate parameters should not be affected by the system parameters or the operating factors of reactor used as far as possible. Furthermore, the model and the parameters employed should favorably explain reduction process under various reducing conditions.

In the reduction of hematite pellets in the stack of the blast furnace, in view of the gas composition and the temperature range, these pellets are primarily reduced to the wustite. This phenomenon may be considered to have an effect on the reduction rate. It is therefore useful to investigate the reduction rate of wustite pellets.

In this connection, the authors applied the equation of reduction rate based on the unreacted core model which takes into account of the three processes to the reduction of hematite pellets and the pellet pre-reduced to wustite, with hydrogen in a high temperature range (850–1,150°C) in order to determine the rate parameters contained in the model and to compare both cases of hematite and wustite pellets. Furthermore, as to reduction curves under various conditions, calculated and measured values were compared to investigate the applicability of the reduction model employed to the reactor analysis.

II. Experiment

1. Sample

Hematite pellets as initial samples with apparent density of 4.12 g/cm^3 and porosity of 0.15 ± 0.01 were supplied from Kobe Steel, Ltd. Table 1. gives the chemical composition of these pellets.

For the pre-reduction of these pellets to the wustite, two types of reducing gas were used; CO-CO_2 and H_2-H_2O gas mixtures. The sample was pre-reduced to the wustite under the conditions of $T=1{,}072$, $p_{CO_2}/p_{CO}=0.40$, $V=30$ and $d_p=1.24$, and slowly cooled in the nitrogen atmosphere, then the physical properties of the

Table 1. Chemical composition of hematite pellets

Element	T·Fe	FeO	SiO_2	CaO	Al_2O_3	MgO	S
wt (%)	65.07	1.37	4.04	0.62	1.23	0.58	0.004

(10) M. Tate, A. Yoshizawa and T. Yamamura: Report of the 54th (Iron-making) Committee, Japan Soc. for the Promotion of Sci. No. 1088 (1967).

(11) M. Amatatsu, M. Fuji, M. Tate, T. Cho and H. Go: Tetsu-to-Hagané, **56** (1970), S. 338.

(12) K. Okabe, T. Hamada and A. Watanabe: Tetsu-to-Hagané, **55** (1969), 764.

sample were measured. Wustite pellets produced in this way had apparent density of 2.85 g/cm^3, porosity of 44% and particle diameter of 1.39 cm. Evidently, the sample swelled and its porosity increased correspondingly from the initial state.

2. Reducing apparatus and procedure

The apparatus shown in Fig. 1 was used for the reducing experiment. High-purity hydrogen was introduced from the gas cylinder into the reaction tube through the autoregulating gage. The flow rate of gas was measured by the gasmeter. The lower portion of the reaction tube was filled with alumina balls and the gas was pre-heated to prevent the temperature drop within the tube.

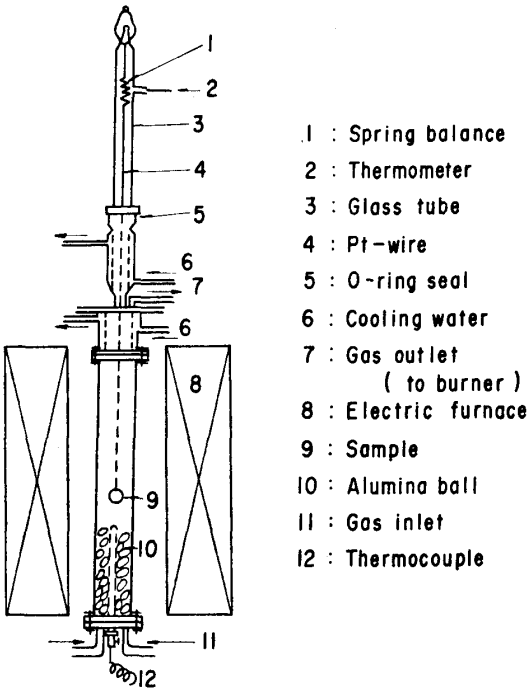

Fig. 1 Experimental apparatus.

The reaction tube of an inside diameter of 7.7 cm was made of heat resisting steel No. 42 of Japan Industrial Standard. This tube installed in the electric furnace using SiC heating elements. The electric furnance was of the vertical type having a height of about 120 cm. Heating was carried on in three stages by the delta connecting method. A constant temperature zone of more than about 40 cm at 950±2°C was obtained. In the reaction tube, a pellet was suspended by a Pt-wire which was connected to a quartz spring (with maximum load of 7 g and sensitivity of 10 mg). The pellet was heated in the nitrogen stream and after reaching the desired temperature, the pellet was reduced by the hydrogen diluted with nitrogen. The decrease in weight during the reduction was read on the cathetometer.

3. Pre-reducing apparatus and procedure

Hematite pellets were pre-reduced to wustite with two types of reducing gas; CO-CO_2 gas mixture from gas cylinders was used, while H_2-H_2O gas mixture was produced by the steam generator shown in Fig. 2.

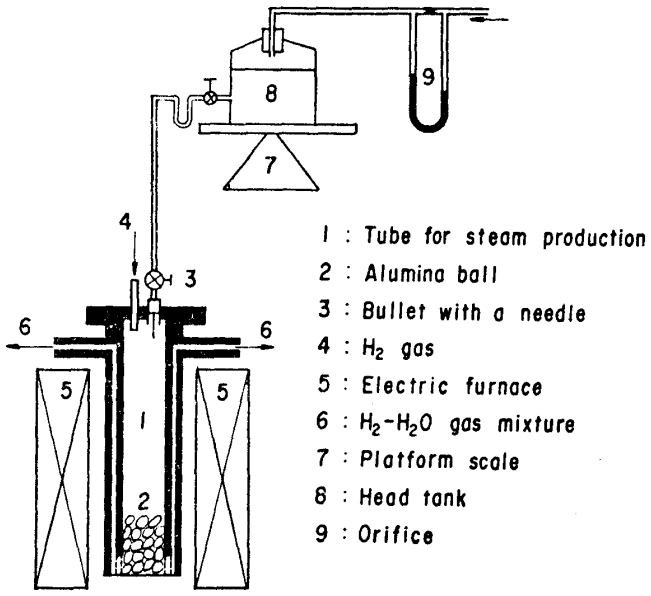

Fig. 2 Steam generator.

The steam generator consists of the concentric tube installed in the electric furance maintained at a constant temperature. Hydrogen flowed into the tube, into which water was also injected. Temperature in the tube was kept constant at 400°C. The pass to the reaction tube shown in Fig. 1 was heated by the baking heater.

The flow rate of the water was regulated by a cock of the burette with a needle at the tip. Complete vaporization of water injected was confirmed by the absorption of steam through water and silica gel. It was also confirmed that the mixture of hydrogen and steam was kept in a specified ratio.

In the pre-reduction of iron oxide pellets to the wustite with CO-CO_2 gas mixture, the wustite pellet was produced which had a composition of $Fe_{0.95}O$ close to the equilibrium; $Fe/FeO/CO$-CO_2. In this case, the ratio of p_{CO_2} to p_{CO} was selected according to the data given by Darken and Gurry[13]. Pre-reducing condition used were fixed to $T=1{,}072$ $p_{CO_2}/p_{CO}=0.40$ and $V=30$. In order to investigate the effect of pre-reducing temperature on properties of wustite, the pre-reduction was conducted at another reducing conditions of $T=859$, $p_{CO_2}/p_{CO}=0.49$ and $V=30$. In comparison of results obtained at two temperatures, no significant difference was found as shown in Fig. 3.

Pre-reduction with H_2-H_2O gas mixture was conducted at $T=1{,}072$, $p_{H_2O}/p_{H_2}=$

(13) L.S. Darken and R.W. Gurry: *Physical Chemistry of Metals* (1953), McGraw-Hill.

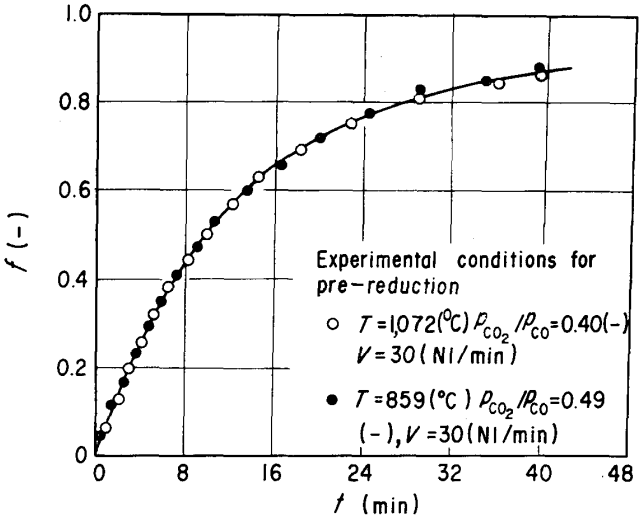

Fig. 3 Effect of the pre-reducing temperature on the reduction curves of wustite pellet Experimental conditions: T=859 (°C), p_{H_2}=1.0 (-), V=50 (N*l*/min), d_p=1.2 (cm).

0.75 and V=30. In this case, in order to obtain the wustite with the same composition as produced with CO-CO_2 gas mixture, the corresponding value of H_2O/H_2 was determined by Eq. (2), which represents the equilibrium constant of the reaction given by Eq. (1)

$$CO+H_2O = CO_2+H_2 \tag{1}$$

$$\log K' = 1{,}880/T-1.67 \tag{2}$$

4. Experimental results

(i) Microscopic examination of reduced sample

Photo. 1- (a) (b) (c) and Photo. 1- (d)(e)(f) show cross-sections of partially reduced pellets in the following cases; in the first case, hematite pellets were reduced under conditions of T=960, p_{H_2}=0.4 (p_{N_2}=0.6), V=50 and d_p=1.2, while in the second case, wustite pellets produced with H_2-H_2O gas mixture were reduced under conditions of T=1,072, p_{H_2}=0.4 (p_{N_2}=0.6), V=50 and d_p=1.3.

In both cases, the reaction proceeded topochemically. In Photo. 1, the boundaries between wustite phase and metallic iron phase, which could be observed very sharply in the case of hematite pellets, while reaction zones are evidently found in the case of wustite pellets. The boundary shown in Photo. 1-(e) was magnified and shown in Photo. 2. The width of reaction zone shown in Photo. 2 was estimated to be about 300 μ which corresponds to about 1/20 of the particle radius. Such a width of reaction zone was due to higher porosity in the pre-reduced wustite pellets than that in the wustite phase appeared during the reduction of the hematite pellet.

The cross-sections of partially reduced pellets at the different temperature was also examined. Results obtained were substantially identical to those shown in Photo. 1.

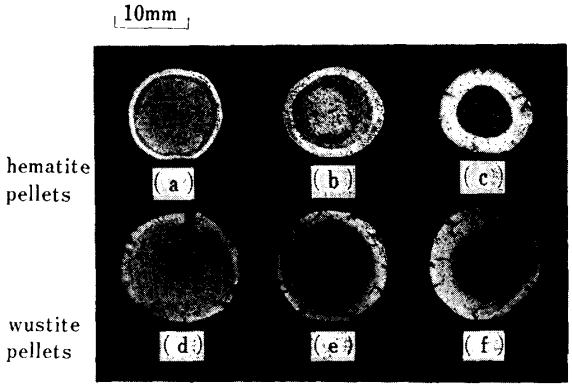

Photo. 1 Cross sections of partially reduced pellets
(a) $f=0.3$ (b) $f=0.5$ (c) $f=0.8$ (d) $f=0.4$ (e) $f=0.6$ (f) $f=0.8$

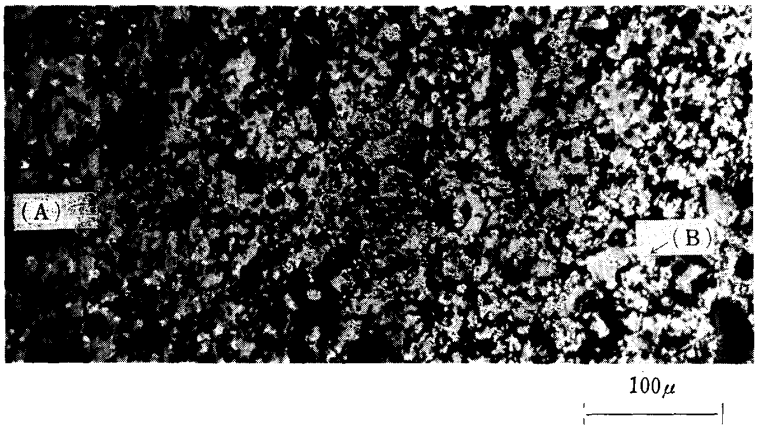

Photo. 2 Reaction interface between wustite and iron for wustite pellet (Photo. 1-(e))
(A) wustite (B) iron

(ii) Reduction curves

Observed values of reduction curves for hematite pellets at various temperatures are shown in Fig. 4, while those for wustite pellets, in Figs. 5 and 6. The observed curves in Fig. 5 corresponds to the case of samples pre-reduced with CO-CO_2 gas mixture and those in Fig. 6 to the case of samples pre-reduced with H_2-H_2O gas mixture. Calculated curves in each figure will be described in detail later. Fractional reduction, f, adopted here is the ratio between oxygen removed in a certain period after the beginning of reduction and total oxygen to be removed. The latter amount was calculated from the sample weight and chemical composition.

III. Equation of reduction rate based on the unreacted core model

Assuming that diffusion through gaseous film, intraparticle diffusion and chemical reaction proceed steadily and successively during the reduction process for the heterogeneous reaction given by Eq. (3) or (4), the overall reduction rate can be represented as Eq. (5),[3]~[8]

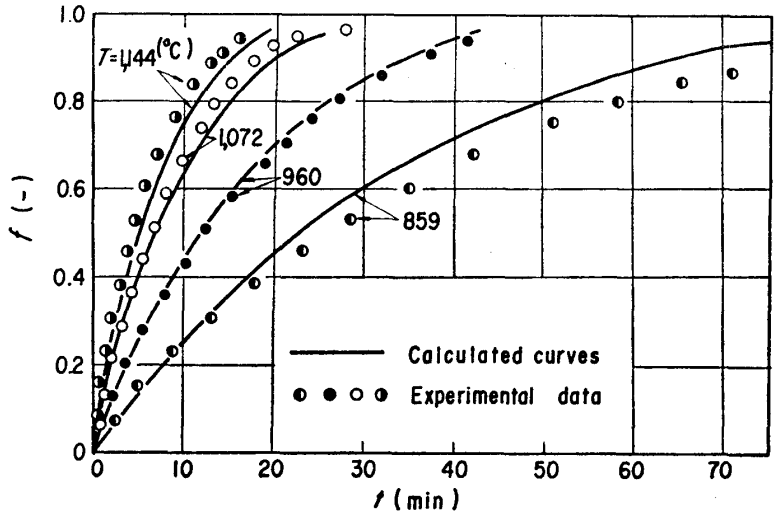

Fig. 4 Comparison of the experimental data with the calculated curves for hematite pellets according to the unreacted core model
Experimental conditions: $p_{H_2}=0.4$ ($p_{N_2}=0.6$) (–), $V=50$ (N*l*/min), $d_p=1.2$(cm).

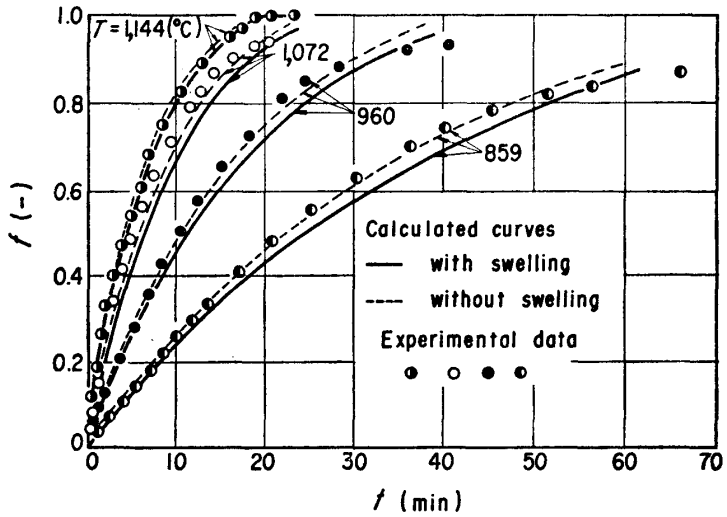

Fig. 5 Comparison of the experimental data with the calculated curves for wustite pellets
Experimental conditions: $p_{H_2}=0.4$ ($p_{N_2}=0.6$) (–), $V=50$ (N*l*/min), $d_p=1.2$ (cm)
Experimental conditions for pre-reduction: $T=1{,}072$ (°C), $p_{CO_2}/p_{CO}=0.40$, $V=30$ (N*l*/min).

$$1/3\,Fe_2O_3+H_2=2/3\,Fe+H_2O \tag{3}$$

$$FeO+H_2=Fe+H_2O \tag{4}$$

$$\bar{R}=(C-C^*)\Big/\frac{1}{4\pi r_0^2}\left\{\frac{1}{k_f}+\frac{r_0(r_0-r_i)}{r_i D_s}+\frac{(r_0/r_i)^2}{k(1+1/K)}\right\} \tag{5}$$

Eq. (5) is integrated and rewritten into Eq. (7) by use of Eq. (6). It is found from Eq. (7) that time, t, required for obtaining a certain fractional reducton, f, is

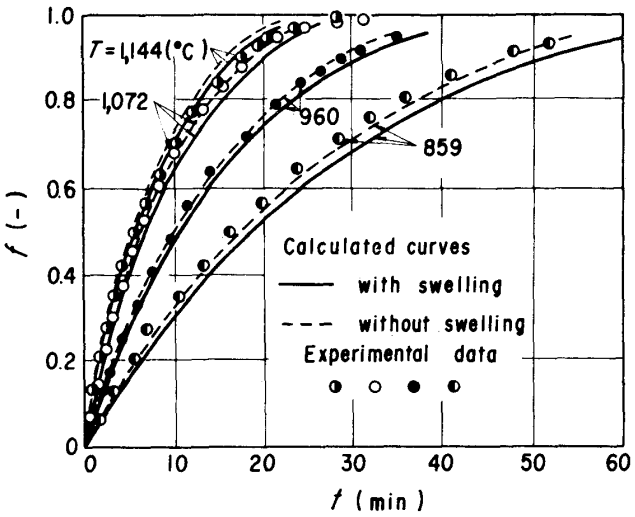

Fig. 6 Comparison of the experimental data with the calculated curves for wustite pellets. Experimental conditions: $p_{H_2}=0.4$ ($p_{N_2}=0.6$) (–), $V=50$ (Nl/min), $d_p=1.3$ (cm) Experimental conditions for pre-reduction: $T=1{,}072$ (°C), $p_{H_2O}/p_{H_2}=0.75$ (–), $V=30$ (Nl/min).

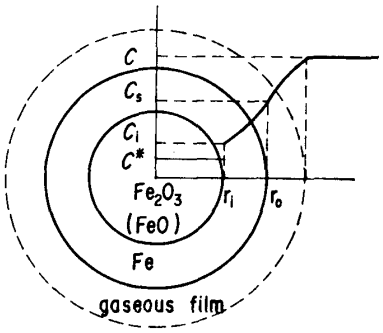

Fig. 7 Unreacted core model

expressed by the sum of respective reduction times controlled by each process.

$$f = 1-(r_i/r_0)^3 \tag{6}$$

$$t = \frac{ad_0r_0}{C-C^*}\cdot\frac{f}{3k_f} + \frac{ad_0r_0^2}{C-C^*}\cdot\frac{1}{6D_s}\{3-3(1-f)^{2/3}-2f\}$$

$$+\frac{ad_0r_0}{C-C^*}\cdot\frac{1-(1-f)^{1/3}}{k(1+1/K)} \equiv t_f+t_d+t_r \tag{7}$$

In Eq. (7), t_f is determined by experimental conditions at a given fractional reduction provided that mass transfer coefficient through gaseous film, k_f, is theoretically estimated. In the present study, k_f was estimated from Ranz-Marshall's equation[14] mentioned later. If t_f, calculated from k_f, is subtracted from both sides of Eq. (7), a relation between fractional reduction and time is obtained under the presence of both resistances of intraparticle diffusion and

chemical reaction. Furthermore, if the values of k and D_s for samples used are known, a reduction curve based on the model can be calculated by Eq. (7).

IV. Determination of the rate parameters

1. Estimation of the mass transfer coefficient through gaseous film.

Mass transfer coefficient through gaseous film, k_f was estimated by Ranz-Marshall's equation(8).[14] Since a diameter of the reaction tube used in the present study was about six times the diameter of sample, Eq. (8) was considered to be satisfied.

$$Sh = 2.0 + 0.6\, Re_p^{1/2} \cdot Sc^{1/3} \tag{8}$$

In Eq. (8), diffusion coefficient of reducing gas, D, was estimated from Andrussow's equation,[15] while the viscosity of gaseous mixture was predicted from Wilke's equation[16] applying the values for respective components calculated from Licht-Stechert's equation.[17] Table 2 shows the values of k_f calculated on the basis of these equations by using experimental conditions shown in Fig. 4. As is clear from this table, values of k_f increase along with the increase in temperature.

Table 2. Calculated values of mass transfer coefficient through gaseous film under the various temperatures in the reduction of hematite pellets

T (°C)	u (cm/min)	d_p (cm)	D (cm²/min)	Re_p (—)	Sc (—)	Sh (—)	k_f (cm/min)
859	4,500	1.20	510	43	0.24	4.5	1,900
960	4,900	1.20	600	41	0.24	4.4	2,200
1,072	5,300	1.19	690	39	0.23	4.3	2,500
1,144	5,600	1.19	770	38	0.23	4.3	2,700

Experimental conditions: $p_{H_2}=0.4$ ($p_{N_2}=0.6$) (—), $D_t=7.7$ (cm), $V=50$ (Nl/min)

Fig. 8 shows reduction curves obtained with the change in the flow rate of gas under the conditions of $T=960$, $d_p=1.2$ and $p_{H_2}=0.4$ ($p_{N_2}=0.6$).

Diffusion resistance through gaseous film was estimated from the value of k_f. This resistance decreases along with the increase in the flow rate of gas. The magnitude of diffusion resistance through gaseous film depends not only upon the flow rate of gas, but also upon other reducing conditions including reduction temperature, component and proportion of diluent gas, and particle diameter.

In certain instances,[9] the resistance caused by the rate of consumption of reducing gas is taken into account in the expression for the overall rate equation.

(14) W.E. Ranz and W.R. Marshall: Chem. Eng. Prog., **48** (1952) 141.
(15) K. Sato: Chem. Eng., Japan, **28** (1964), 490.
(16) C.R. Wilke: J. Chem. Phys., **18** (1950), 517.
(17) W. Licht and D.G. Stechert: J. Phys. Chem., **48** (1944), 23.

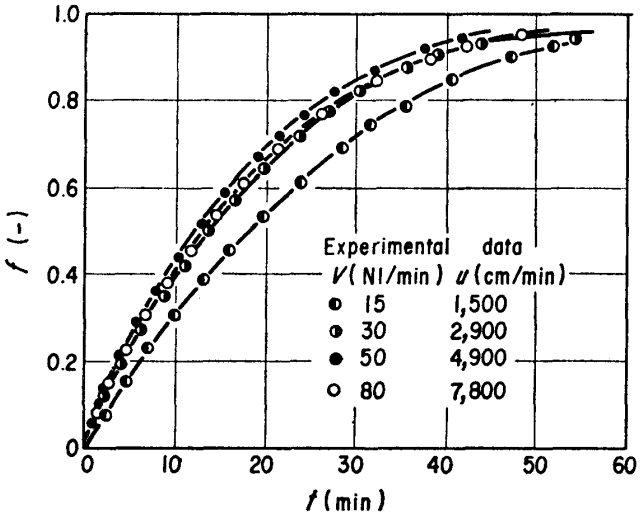

Fig. 8 Effect of the flow rate of gas on the reduction curves of hematite pellets
Experimental conditions: T=960 (°C), p_{H_2}=0.4 (p_{N_2}=0.6) (–), d_p=1.2 (cm)

However, the resistance calculated in such a way may be doubtful whether it is equivalent to other resistances. Therefore the resistance mentioned above was neglected in the present study. However this resistance, expressed by the term of $4\pi r_0^2/Q$, was tried to calculated under the conditions of T=960 and V=50. The ratio of this resistance to the sum of this resistance and diffusion resistance through gaseous film was 5% or less. Accordingly, the resistance caused by the rate of consumption of reducing gas could be neglected under these conditions.

2. Reaction rate constant

Reaction rate constant, k, was determined by the application of observed data to the method by mixed control proposed by Yagi and Ono[5]. The graphical representation of observed data of hematite pellets was shown in Fig. 9. Data in a higher temperature present a relatively good linear relation, while those in a lower temperature tend to progressively lose the linearity. The value of k was calculated from values of the intercept of straight lines drawn in Fig. 9.

The temperature dependence of k obtained is shown in Fig. 12 and expressed by Eq. (9), then the activation energy of k is about 26 kcal/mol. This activation energy is slightly higher than previously reported values which were obtained by other researchers in assuming the chemical reaction control.

$$k = \exp\,(16.2-25.7\times10^3/RT) \qquad (9)$$

Fig. 10 shows mixed control plots of observed data for wustite pellets pre-reduced with CO-CO_2 gas mixture. In Fig. 10, observed data at T=1,144 present the linear relation with a slope, while those at other temperatures become progressively drawn in horizontal line along with the decrease in reducing temperature. This means that, at a lower reducing temperature, the resistance of

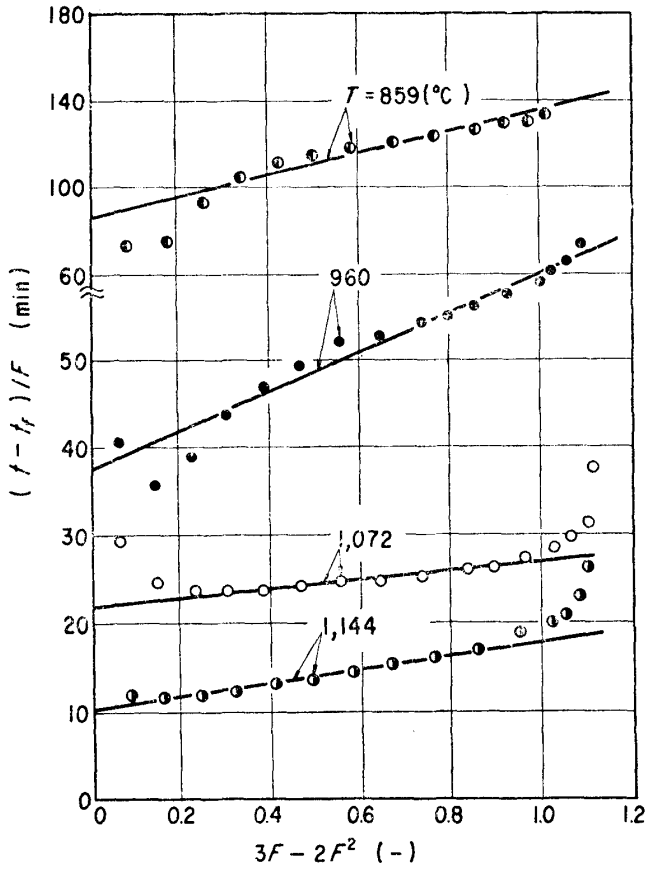

Fig. 9 Plots of the experimental data for hematite pellets by $(t\text{-}t_f)/F$ vs. $3F\text{–}2F^2$
Experimental conditions: $p_{H_2}=0.4$ ($p_{N_2}=0.6$) (–), $V=50$ (Nl/min), $d_p=1.2$ (cm).

diffusion decreased to a negligible value and the ratio of resistance of chemical reaction to overall resistance became relatively large, so that observed data behaved as the chemical reaction control. On the other hand, in the case of $T=$ 1,144, it may be considered that the higher reduction temperature led to the lower resistance of chemical reaction and the higher resistance of diffusion relatively. Therefore, the observed data may be explained by the mixed control.

Fig. 11 shows mixed control plots of observed data for wustite pellets pre-reduced with H_2-H_2O gas mixture. In this case, observed data in a higher temperature range lay almost on a straight line, however, those in lower temperature tends to deviate from linear relation. The result shown in Fig. 11 is distinguished from that in Fig. 10, having a slope at any reducing temperature.

Temperature dependence of k for wustite pellets are shown in Fig. 12. The expression for k is given by Eqs. (10) and (11) respectively.
Pre-reduction with CO-CO_2 gas mixture:

$$k = \exp\,(15.9-26.2\times 10^3/RT) \tag{10}$$

Pre-reduction with H_2-H_2O gas mixture:

$$k = \exp\,(13.9-20.5\times 10^3/RT) \tag{11}$$

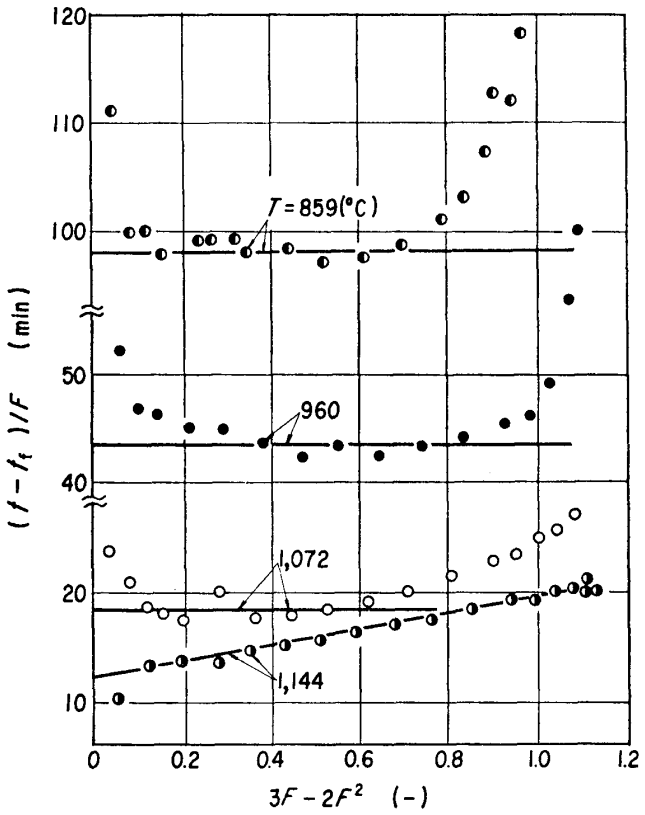

Fig. 10 Plots of the experimental data of wustite pellets by $(t-t_f)/F$ vs. $3F-2F^2$
Experimental conditions: $p_{H_2}=0.4$ ($p_{N_2}=0.6$) (-), $V=50$ (N*l*/min), $d_p=1.2$ (cm)
Experimental conditions for pre-reduction: $T=1{,}072$ (°C), $p_{CO_2}/p_{CO}=0.40$ (-), $V=30$ (N*l*/min).

The activation energy slightly varies with pre-reducing conditions.

A comparison between cases of hematite pellets and wustite pellets shown in Fig. 12 illustrates that the value of k for hematite pellets is slightly higher, while the activation energy is somewhat lower in Eq. (11). However, in view of the precision of activation energy obtained from the experiments for gas-solid reaction, it may be considered that there are no significant differences among three cases.

In the evaluation of the reaction rate constant, equilibrium constant, K, of the reactions of Eqs. (3) and (4) was calculated from Eq. (12) obtained from thermodynamic data[18] of equilibrium relation between wustite and iron:

$$K = \exp(1.0837 - 1{,}737.2/T) \tag{12}$$

3. Estimation of the intraparticle diffusion coefficient

Intraparticle diffusion coefficient, D_s, can be obtained from the slope of the mixed control plot of observed data. However, as is shown in Figs. 9, 10 and 11,

(18) O. Kubaschewski, E. LL. Evans and C.B. Alcock: *Metallurgical Termochemistry*, Fourth ed., (1967), Pergamon Press.

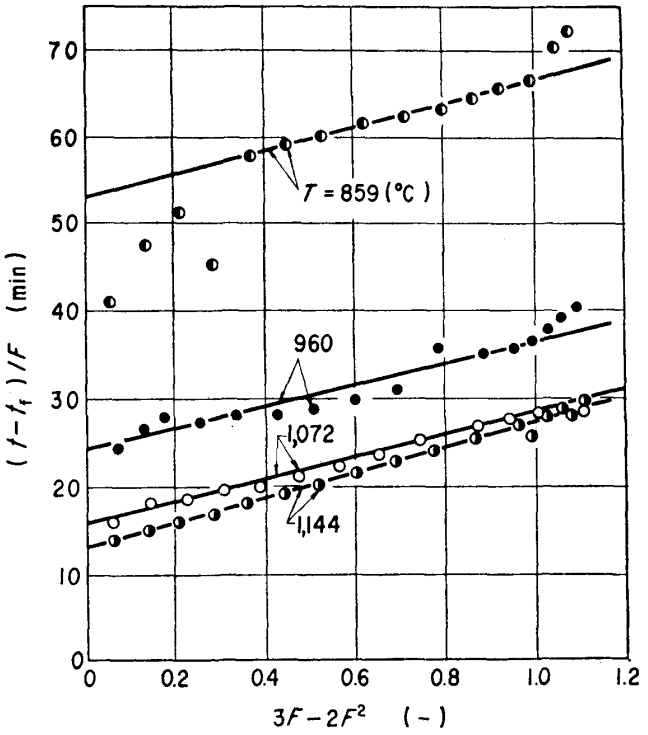

Fig. 11 Plots of the experimental data for wustite pellets by $(t\text{-}t_f)/F$ vs. $3F\text{-}2F^2$
Experimental conditions: $p_{H_2}=0.4$ ($p_{N_2}=0.6$) (-), $V=50$ (Nl/min), $d_p=1.3$ (cm)
Experimental conditions for pre-reduction: $T=1{,}072$ (°C), $p_{H_2O}/p_{H_2}=0.75$ (-), $V=30$ (Nl/min).

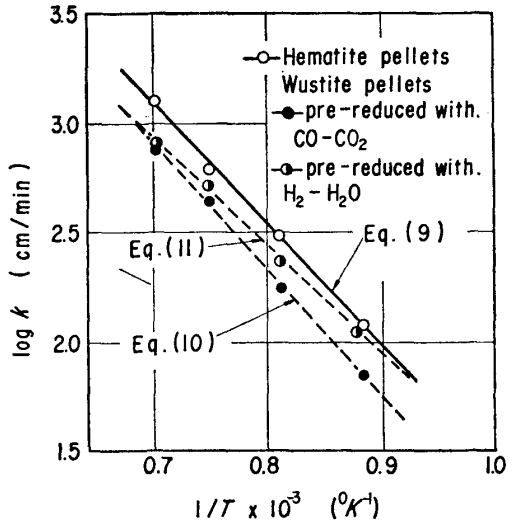

Fig. 12 Temperature dependence of reaction rate constant.

the linear relation of such plots is not always satisfactory. Accordingly, it is difficult to determine D_s from slopes of these plots. In these circumstances, D_s was theoretically estimated from Eq. (13).

$$D_s = \varepsilon_f \cdot \xi \cdot D \tag{13}$$

In this equation, ε_f is related to ε_p (or ε_w) as presented by Eq. (14), provided that the particle diameter does not vary during the reduction. Value of ξ was estimated by Eq. (15) obtained from experimental data reported by Olsson and McKewan,[19] and Hara et al.[20]

$$\varepsilon_f = 0.534 + 0.466\,\varepsilon_p \text{ (or } \varepsilon_w) \tag{14}$$

$$\xi = 4.4\times10^{-4}\,(T-773) + 0.18 \tag{15}$$

$$(T \geqq 773\,°\mathrm{K})$$

In order to examine experimental equation (15), D_s was calculated from slopes of mixed control plots shown in Figs. 9, 10 and 11, ξ was calculated by Eqs. (13) and (14). Comparison of the values for ξ obtained with Eq. (15) are shown in Fig. 13. As is clear from this figure, values of ξ thus determined were almost identical to those obtained from Eq. (15) except the case of $T=1{,}072$. It should however be mentioned here that only the data in the case of $T=1{,}144$ were adopted from Fig. 10.

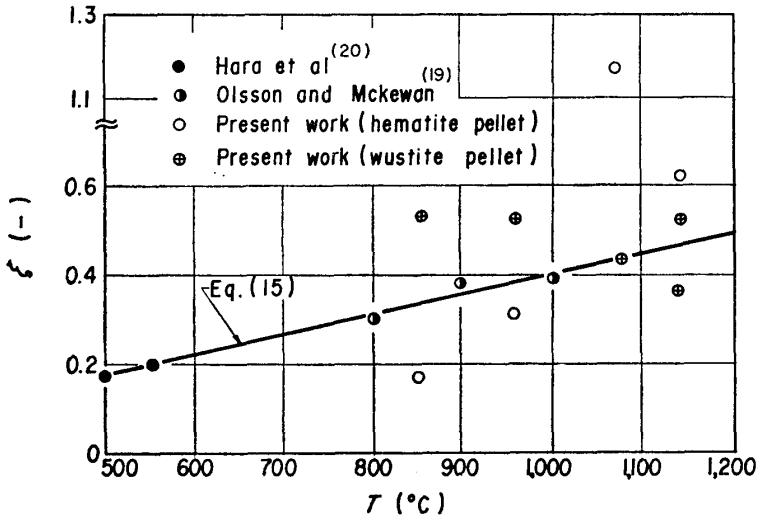

Fig. 13 Relation between labyrinth factor and temperature.

Initial porosity, ε_w, of wustite pellets was estimated from Eq. (16) derived on the assumption that initial wustite pellets had the same particle diameter as initial hematite pellets.

$$\varepsilon_w = 1 - \frac{d_a}{d_w} \qquad (d_w = 5.67) \tag{16}$$

When the porosity of initial hematite pellet is 15%, that of wustite pellet calculated from Eq. (16) is equal to 32%. On the other hand, as stated in the previous paragraph, the porosity of the wustite pellet actually measured is equal

(19) R.G. Olsson and W.M. McKewan: Trans. Met. Soc. AIME, **236** (1966), 1518.
(20) Y. Hara, M. Sugata, T. Kaida and S. Kondo: J. Japan Inst. Metals, **31** (1967), 207.

to 44%. This difference in porosity is due to the particle expansion. Strictly, the effect of this expansion on the overall reduction rate should be considered. This subject will be described later in detail.

4. Evaluation for resistance of each process

As is expressed by Eq. (5), the overall reduction rate derived on the basis of the unreacted core model includes resistances of three processes. The resistance of each process was theoretically studied by Moriyama et al.[4] In this study a similar method was adopted. In other words, rate parameters obtained was used and ratios of respective resistances represented by individual terms of the denominator in the right side of Eq. (5) to the overall resistance were calculated from the observed data shown in Fig. 4. Results obtained are shown in Fig. 14.

In Fig. 14, both ratios of diffusion resistance through gaseous film and of reaction resistance to the overall resistance decrease along with the progress of reduction, while the ratio of resistance of intraparticle diffusion increases. These results

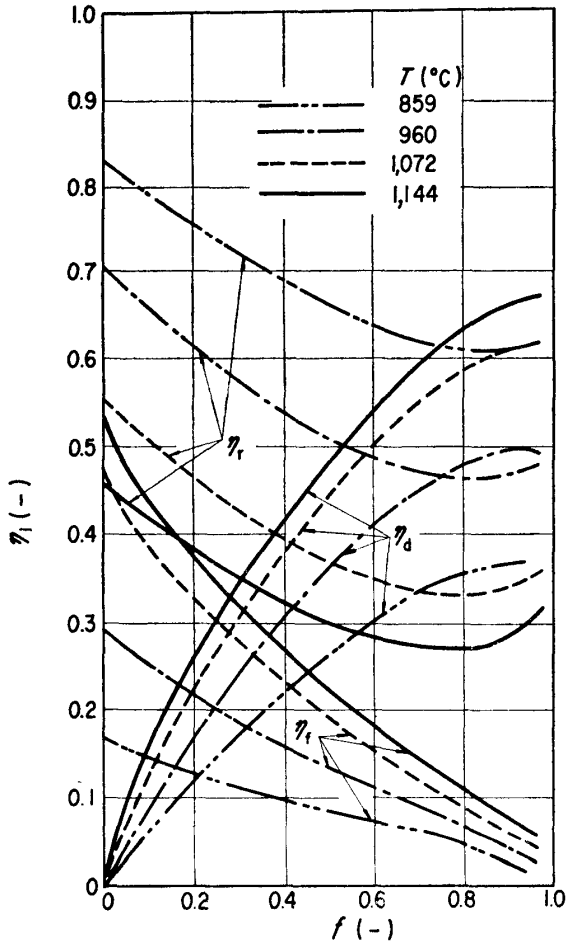

Fig. 14 Resistance of each process of diffusion through gaseous film, intraparticle diffusion and chemical reaction for the reduction of hematite pellets

show a tendency similar to those of Moriyama et al.[4] For the observed data of wustite pellets, almost same results were obtained.

It is found from Fig. 14 that the effect of resistance of diffusion through gaseous film is important, particularly at a higher reducing temperature and in an initial stage of reduction. Consequently, the resistance of diffusion through gaseous film should be evaluated with accuracy.

V. Effect of concentration of reducing gas and particle diameter on reduction rate of hematite pellet

The useful reduction model should be able to express the overall reduction rate of the pellet under various conditions. In the present study, the effect was examined of the concentration of reducing gas and the particle diameter on the reduction rate of hematite pellet, which were considered as the important factors in the model.

As to the effect of the dilution of reducing gas with nitrogen on the reduction rate, it has been reported that the rate decreases due to the adsorption of nitrogen on the reaction interface,[21] or due to the change in the resistance of intraparticle diffusion.[22] In this paper, it was examined whether the reduction rate was of the reversible first order with respect to the concentration of reducing gas or not, as expressed in Eq. (5).

Fig. 15 shows observed reduction curves in the case where the reducing gas was diluted with the nitrogen in various proportions under the reducing conditions of $T=960$, $d_p=1.2$ and $V=50$.

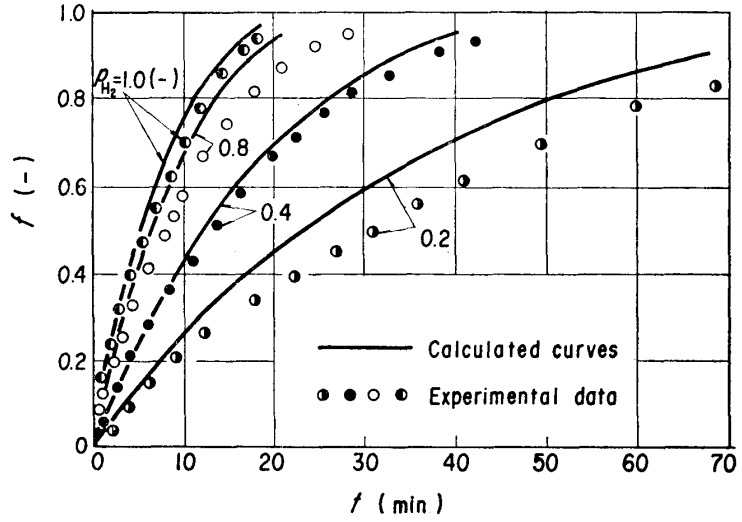

Fig. 15 Comparison of the experimental data with the calculated curves of hematite pellets under the various compositions of reducing gas.
Experimental conditions: $T=960$ (°C), $V=50$ (Nl/min), $d_p=1.2$ (cm)

(21) W.M. McKewan: J. Metals, **16** (1964), 781.
(22) N.A. Warner: Trans. Met. Soc. AIME, **230** (1964), 163.

Provided that the reduction rate is of reversible first order with respect to the concentration of reducing gas, plots of log $(t\text{-}t_f)$ vs. log $(C\text{-}C^*)$ can be expressed by the straight line with a slope of -1 at a constant value of f. Fig. 16 represents plots of log $(t\text{-}t_f)$ vs. log $(C\text{-}C^*)$. From Fig. 16, observed data shows the linear relation at any fractional reduction. The slopes of such a straight lines are nearly equal to -1. These results shows that reversible first order mentioned above is reasonable.

Fig. 17 represents the reduction curves for the case where the particle diameter was changed under the reducing conditions of T=960, p_{H_2}=0.4 (p_{N_2}=0.6) and V=50.

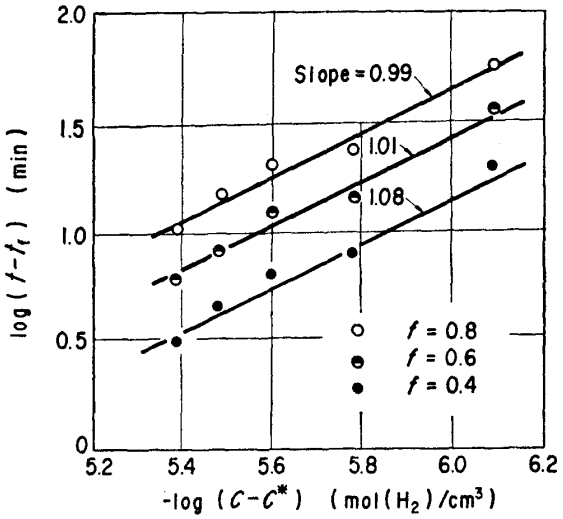

Fig. 16 Relations between log $(t\text{-}t_f)$ vs. log $(C\text{-}C^*)$ at the given fractional reduction of hematite pellets.

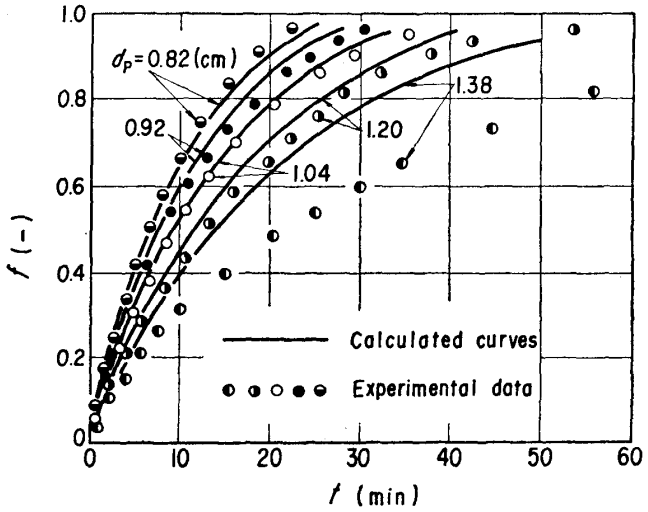

Fig. 17 Comparison of the experimental data with the calculated curves under the various diameters of hematite pellets.
Experimental conditions: T=960 (°C), p_{H_2}=0.4 (p_{N_2}=0.6) (-), V=50 (Nl/min)

Calculated curves shown in Figs. 15 and 17 will be mentioned in detail later.

VI. Applicability of reduction rate and rate parameters

A number of attempts have been made by many investigators to determine the rate parameters on the basis of the reduction model proposed. However, only a few authors have applied the parameters obtained to the reduction model and compared the reduction curves calculated from the various reducing conditions with observed data to examine the applicability of the model and the rate parameters. In this paper, the rate parameters determined in the previous way were applied to Eq. (7) and the reduction curves under various reducing conditions were calculated.

1. Variations of temperature, concentration of reducing gas and particle diameter in the reduction of hematite pellet

Fig. 4 shows a comparison of observed data with calculated reduction curves. It is clear that calculated curves agree well with observed data. At certain temperatures, however, a difference of about 5% is found between both values. This difference may be considered from the accuracy of temperature dependence for k obtained from observed data. On the whole, calculated curves and observed data may be considered to be in a satisfactory agreement.

Figs. 15 and 17 show the comparisons in the cases of various concentration of reducing gas and particle diameter respectively. With the exception of the results obtained at $d_p=1.38$ shown in Fig. 17, calculated curves agree practically with observed data in both cases.

It is found from these results that the reduction model employed may express the effects of variations in temperature, concentration of reducing gas and particle diameter on the reduction curve.

2. Variation of temperature in the reduction of wustite pellet

Figs. 5 and 6 show a comparison of calculated reduction curves with observed data in the case of the pre-reduction to the wustite with CO-CO_2 and H_2-H_2O gas mxitures respectively. As mentioned previously, the pre-reduced wustite pellet swelled and correspondingly increased in porosity as compared with the initial hematite pellet. Calculated curves shown in Fig. 5 correspond to two cases with and without considering the swelling, the former is given by the solid line, while the latter is given by the broken line. The solid line was calculated by the use of measured value ($\varepsilon_w=0.44$) of samples pre-reduced with CO-CO_2 gas mixture. The broken line was calculated by the use of the theoretical value of the porosity ($\varepsilon_w=0.32$) expressed by Eq. (16). However, a comparison of calculated curves with observed data presents a satisfactory agreement of these two cases. As a result, the reduction model and the rate parameters obtained sufficiently expresses also the reduction rate of pellets pre-reduced to the wustite.

Results obtained for pellets pre-reduced with H_2-H_2O gas mixture shown in Fig. 6 have the same tendency as with CO-CO_2 gas mixture. In this case, the measured value of porosity of the wustite pellet was 39%, thus being slightly smaller than that of the pellet pre-reduced with CO-CO_2 gas mixture.

3. Changes of experimental conditions during the reduction of hematite pellets

In order to examine whether or not the reduction model and its rate parameters mentioned in the preceding paragraph can express the reduction rate under nonisothermal conditions, calculated curves were compared with observed data, in the case that one of the experimental conditions was altered during the reduction. Eq. (17) can be derived from Eq. (5) by use of Eq. (6).

$$\frac{1}{3}\int_0^f \left[\alpha\beta+\alpha\left\{(1-f)^{-1/3}-1\right\}+\frac{1}{\delta}(1-f)^{-2/3}\right]df=\int_0^\theta d\theta \tag{17}$$

where, $\alpha \equiv kr_0/D_s$, $\beta \equiv D_s/r_0k_f$, $\delta \equiv 1+1/K$ and $\theta \equiv d_0k(C-C^*)t/3r_0$ (18)

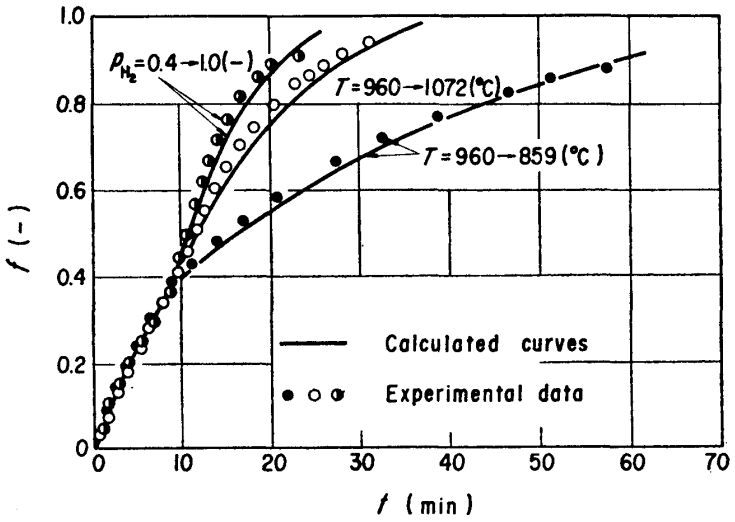

Fig. 18 Comparison of the experimental data with the calculated curves in the case where one of the reducing conditions was altered during the reduction.
Experimental conditions: T=960 (°C), p_{H_2}=0.4 (p_{N_2}=0.6) (-), V=50 (Nl/min), d_p=1.2 (cm)

By integrating Eq. (17), Eqs. (19) and (20) are derived as the relation between θ and f in a case where one of the reducing conditions is altered at $\theta=\theta_0$.

$$\theta=\frac{\alpha}{3}(\beta-1)f+\frac{\alpha}{2}\left\{1-(1-f)^{2/3}\right\}+\frac{1}{\delta}\left\{1-(1-f)^{1/3}\right\} \tag{19}$$

$(\theta \leqq \theta_0)$

$$\theta=\frac{\alpha_1}{3}(\beta_1-1)f-\frac{\alpha_1}{2}(1-f)^{2/3}-\frac{1}{\delta}(1-f)^{1/3}+F_0+F_1 \tag{20}$$

$(\theta > \theta_0)$

where,

$$F_0 = \frac{\alpha}{3}(\beta-1)f_0 + \frac{\alpha}{2}\{1-(1-f)^{2/3}\} + \frac{1}{\delta}\{1-(1-f_0)^{2/3}\} \quad (21)$$

$$F_1 = \frac{\alpha_1}{3}(\beta_1-k)f_0 + \frac{\alpha_1}{2}(1-f_0)^{2/3} + \frac{1}{\delta}(1-f_0)^{1/3} \quad (22)$$

Fig. 18 represents a comparison between curves calculated from Eqs. (19) and (20) and observed data. In all cases, both values agree well with each other.

Observed data shown in Fig. 18 are the results obtained by using the samples which were kept in the nitrogen stream after the reduction for 9 minutes under the conditions of $T=960$, $p_{H_2}=0.4$ ($p_{N_2}=0.6$), $V=50$ and $d_p=1.2$, with the subsequent change in one of these conditions to a specified level.

VII. Conclusion

Hematite pellets and iron oxide pellets pre-reduced to wustite were reduced with hydrogen under various reducing conditions in the temperature range from 850 to 1,150°C. Applicability of the reduction rate based on an unreacted core model to the experimental results was examined and the following information was obtained.

(1) In the reduction of iron oxide pellets, the reaction proceeds topochemically. In the case of hematite pellets, a sharp interface was found between wustite and metallic iron phases by macro- and microscopic observation. In the case of wustite pellets, however, reaction zone was found.

(2) In the case of a higher temperature and the initial stage of reduction, the diffusion resistance through gaseous film has an considerably great effect.

(3) As to the reaction rate constant and the activation energy, there is no significant difference between the reduction of hematite pellets and that of wustite pellets.

(4) If the rate parameters determined by the present method are employed, the reduction rate of hematite pellets with the variation of various conditions including reducing temperature, concentration of reducing gas and particle diameter can be expressed by the reduction model used in the present study. Reduction rate of wustite pellets with an increased porosity can also be expressed by this model.

Further studies will be required on the method for the evaluation of the diffusion resistance through gaseous film and the physical properties of wustite pellets.

Acknowledgements

The authors wish to thank The Central Research Institute of Kobe Steel Ltd. for their kind supply of samples. They would also like to express their apprecia-

tion to H. Shimamura of Kawasaki Steel Corp., Research Laboratories and T. Terui, technician of the Research Institute of Mineral Dressing and Metallurgy, Tohoku University.

Nomenclature

a	stoichiometric coefficient (1 for wustite, 3 for hematite)
C	bulk concentration of reducing gas (mol H_2/cm^3)
C^*, C_i, C_s	concentration of reducing gas at equilibrium state, reaction interface and surface of the pellet, respectively (mol H_2/cm^3)
D	diffusion coefficient of reducing gas (cm^2/min)
D_s	intraparticle diffusion coefficient of reducing gas (cm^2/min)
D_t	inner diameter of reaction tube (cm)
d_a	apparent density of wustite pellet (g/cm^3)
d_0	apparent molar density of hematite and wustite pellets (mol Fe_2O_3/cm^3), (mol FeO/cm^3)
d_p	diameter of pellet (cm)
d_t	density of hematite (g/cm^3)
d_w	density of wustite (g/cm^3)
F	$=1-(1-f)^{1/3}$ (–)
f	fractional reduction (–)
K, K'	equilibrium constants of Eqs. (4) and (1), respectively (–)
k	reaction rate constant (cm/min)
k_f	mass transfer coefficient through gaseous film (cm/min)
p_{H_2}, p_{N_2}	partial pressures of hydrogen and nitrogen, respectively (–)
Q	flow rate of gas (cm^3/min)
R	gas constant (cal/°K.mol)
$\bar{R}$	rate of reduction (mol H_2/min)
Re_p	Reynolds number based on the particle diameter ($=d_p u\rho/\mu$) (–)
r_i, r_0	radius of unreacted core and radius of pellet, respectively (cm)
Sc	Schmidt number ($=\mu/\rho D$) (–)
Sh	Sherwood number ($=k_f d_p/D$) (–)
T	temperature (°C)
$\boldsymbol{T}$	temperature (°K)
t	reduction time (min)
t_f, t_d, t_r	reduction time controlled by respective processes of diffusion through gaseous film, intraparticle diffusion and chemical reaction, respectively (min)
u	linear velocity of gas (cm/min)
V	flow rate of gas (Nl/min)
W	weight of a pellet (g)
α, β, δ, θ	dimensionless terms of Eq. (18) (–)

ε_f	porosity of reduced layer (–)
ε_p	porosity of hematite pellet (–)
ε_w	porosity of wustite pellet (–)
η_f, η_d, η_r	ratios of the resistance of diffusion through gaseous film, intraparticle diffusion and chemical reaction to the overall resistance, respectively (–)
μ	viscosity of reducing gas (g/cm·min)
ξ	labyrinth factor (–)
ρ	density of reducing gas (g/cm^3)